Accepted Article

This manuscript has been accepted after peer review and appears as an Accepted Article online prior to editing, proofing, and formal publication of the final Version of Record (VoR). This work is currently citable by using the Digital Object Identifier (DOI) given below. The VoR will be published online in Early View as soon as possible and may be different to this Accepted Article as a result of editing. Readers should obtain the VoR from the journal website shown below when it is published to ensure accuracy of information. The authors are responsible for the content of this Accepted Article.

COMMUNICATION

The significance of metal coordination in imidazole-functionalized metal organic frameworks for carbon dioxide utilization

William R. Webb[ac], Matthew E. Potter[a], Daniel J. Stewart[a], Stuart J. Elliott[a,f], Pier J. A. Sazio[b], Zhongxing Zhang[c], He-Kuan Luo[c], Jinghua Teng[c], Liling Zhang[d], Chiara Ivaldi[e], Ivana Miletto[e], Enrica Gianotti[e] and Robert Raja[a*]

Abstract: The grafting of imidazole species onto coordinatively unsaturated sites within metal organic framework MIL-101(Cr) enables enhanced CO_2 capture in close proximity to catalytic sites. The subsequent combination of CO_2 and epoxide binding sites, as shown through theoretical findings, significantly improves the rate of cyclic carbonate formation, producing a highly active CO_2 utilization catalyst. An array of spectroscopic investigations, in combination with theoretical calculations reveal the nature of the active sites and associated catalytic mechanism which validates the careful design of the hybrid MIL-101(Cr).

Metal organic frameworks (MOFs) have shown great potential for carbon capture. Furthermore, they can facilitate the utilization of sequestered CO_2 to produce value-added chemicals.[1–3] MIL-101(Cr),[4] a chromium-based terephthalate MOF, is of particular interest, due to the coordinatively unsaturated sites (CUS) on the metal nodes, which can induce CO_2 adsorption.[5] The high thermal stability (up to 275 °C) coupled with large pores (29 and 34 Å) and pore windows (12 and 14.7x16 Å) makes MIL-101(Cr) attractive from a catalytic perspective, permitting large substrates and elevated temperatures.[4] The metal sites in MIL-101(Cr) can be suitably manipulated for post synthetic modification (PSM) of the framework, including grafting amine ligands,[6,7] leading to the generation of isolated catalytic sites.[8,9] MOFs have recently been employed for the production of cyclic carbonates (precursors for polyurethanes and polycarbonates) from CO_2, however, a large majority require a halide co-catalyst or solvent, long reaction times (greater than 24 hours) or both.[10–13] To date, few examples of MOF-based catalysts exist which are capable of this transformation without additional reagents. A review of these MOFs and their reaction conditions are summarized in the supporting information (Table S1). Imidazoles can catalyze the production of cyclic carbonates *via* CO_2 incorporation and have been previously shown to activate MOFs towards CO_2 insertion, through their installation onto the organic linker, via PSM or mixed-ligand approaches, to produce imidazolate functionalities balanced by halides.[14–17] Although providing potential of converting epoxides to their associated carbonate counterparts under 1 bar CO_2 pressure, imidazole-

[a]School of Chemistry, University of Southampton, Southampton SO17 1BJ, UK. *Corresponding author: Prof Robert Raja, r.raja@soton.ac.uk
[b]Optoelectronics Research Centre, University of Southampton, Southampton SO17 1BJ, UK
[c]Institute of Materials Research and Engineering (IMRE), Agency for Science, Technology and Research (A*STAR), Innovis, 2 Fusionopolis Way, Singapore 138634.
[d]Institute for High Performance Computing (IHPC), Agency for Science, Technology and Research (A*STAR), #16-16 Connexis (North), 1 Fusionopolis Way, Singapore 138632.
[e]Department of Science and Technological Innovation, Università del Piemonte Orientale, Viale T.Michel 11, 15121, Alessandria, Italy.
[f]Centre de Résonance Magnétique Nucléaire à Très Hauts Champs - FRE 2034 Université de Lyon / CNRS / Université Claude Bernard Lyon 1 / ENS de Lyon, 5 Rue de la Doua, 69100 Villeurbanne, France

Supporting information for this article is given via a link at the end of the document.

containing linkers require intense synthetic prerequisites (Table S1).

Similar in strategy to that described by Xiao and coworkers, well-defined CUS sites inherent to the MIL-101 architecture offer an unique opportunity to graft functionalized imidazoles directly to the metal node, removing lengthy synthetic requirements, and ensuring precise site-isolation and loading of imidazoles to serve as active sites in the conversion of CO_2 to cyclic carbonates.[18] In doing so, the necessity of additional reagents is removed, and catalysis can be performed under significantly shorter reaction times and pressure, compared to that previously reported for this catalyst design rationale.

In this study, a range of imidazoles were grafted onto MIL-101(Cr) (Figures 1, S1 and Table S2) via PSM, with loadings of 1.0 mmol g^{-1} (Table S3). However, we now focus on 1-methyl imidazole (MIL-101-Me) due to its commercial availability and ease of characterization. The bare MIL-101(Cr) species shows a crystalline diffraction pattern (Figure S2), uniform sized and shaped crystals (Figure S3), porosity (Figure S4) and thermogravimetric data (Figure S5), all in excellent agreement with the literature, confirming the structural and textural integrity of our material.[4,6] On introducing the imidazole (MIL-101-Me) we see no significant variation in XRD pattern (Figure S2), crystal topology (Figure S3B) or thermal stability (Figure S5). However, the pore volume and surface area of the material decreased, as the imidazoles occupy the framework (Figure S4). This confirmed that the incorporation of the imidazole preserved the physicochemical characteristics of the MIL-101(Cr) framework.
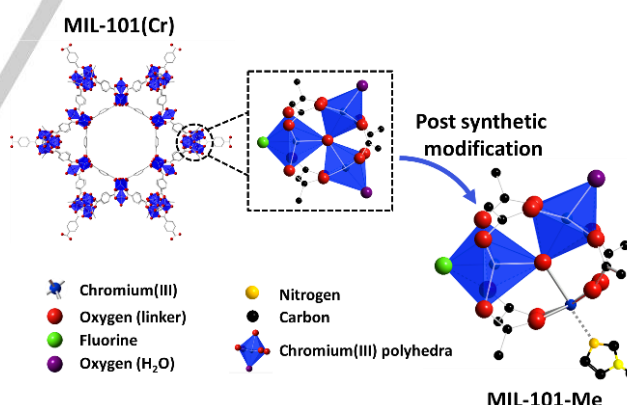

Figure 1: Graphical representation of 1-methyl imidazole grafting to CUS of MIL-101(Cr) through replacing the water ligand.

The EPR spectrum of bare MIL-101(Cr) (Figure S6, green) is in good agreement with the literature, showing a broad line shape centered at ~3500 G, indicative of high spin Cr^{3+} in a pseudo-octahedral environment.[8] The broadening is attributed to the lack of symmetry in the ligands around chromium, and the number of crystallographically distinct chromium sites in MIL-101(Cr). The MIL-101-Me EPR spectrum (Figure S6, black) is noticeably broader, indicating a change in the electron spin–spin state of the chromium species. This is likely due to modification of neighboring nuclei,[7] and a reduction in symmetry due to the addition of a new ligand (potentially the imidazole).

COMMUNICATION

These findings are corroborated with DR UV-Vis spectroscopy (Figures 2 & S7). The spectra of MIL-101(Cr) and MIL-101-Me (dotted curves), in air, in the vis region (Figure S7A), shows two d-d transitions; 22270 and 16420 cm^{-1} typical of pseudo-octahedral Cr^{3+}.[19,20] In the UV region, charge transfer and ligand centered transitions are also present (Figure S7B). Outgassing to remove physisorbed water (as shown by the removal of the 5320 cm^{-1} band in the NIR spectra, Figure S8),[21] at 150 °C (solid curves), increases the intensity of the d-d transitions, which becomes broader, with shoulders appearing at lower wavenumbers. Notably a shoulder at ~13600 cm^{-1} is visible and a new band at ~10280 cm^{-1} appears, assigned to CUS Cr^{3+} sites.[19,22] In MIL-101-Me the d-d bands are blue-shifted with decreased intensities. Further, the shoulders appear less prominent, due to the presence of a strong field ligand on Cr^{3+} sites, such as the imidazole.[23] CO_2 adsorption on unsaturated Cr^{3+} sites at room temperature was observed with DR UV-Vis spectroscopy (Figure 2). For MIL-101(Cr), the shoulder at 13600 cm^{-1} disappears and the band at 10280 cm^{-1} is partially eroded. The same behavior is also observed for MIL-101-Me. The CO_2 coordination on Cr^{3+} Lewis sites is almost irreversible by outgassing the samples at room temperature; CO_2 can be removed completely upon outgassing the materials at 150 °C (Figure S9).
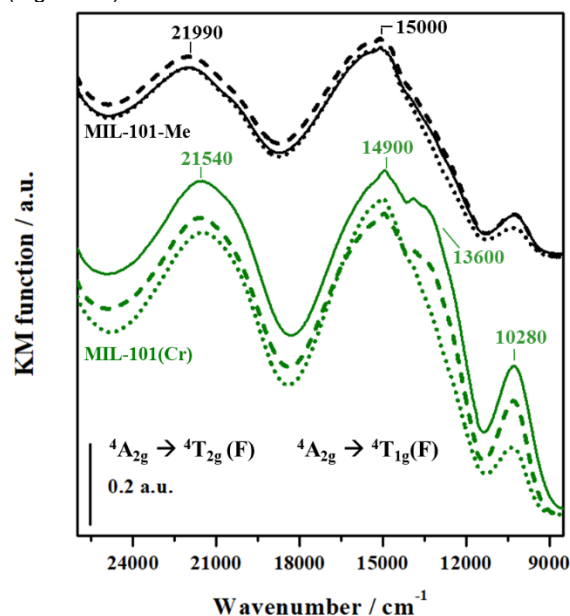
interacts with residual OH groups.[25] The band at 2318 cm^{-1} is associated with acetonitrile coordinated with CUS Lewis acid sites (Cr^{3+}).[26] By decreasing the acetonitrile pressure, a shoulder appears at 2312 cm^{-1}. These two components (2312 and 2318 cm^{-1}) indicate that two Cr^{3+} un-coordinated Lewis acid sites with different strength are present, in agreement with the DR UV-Vis spectra. The adsorptions of CD_3CN on Cr^{3+} sites are less intense for MIL-101-Me, as the grafted imidazole blocks the Cr^{3+} CUS. Both materials, show a shift (Δv_{CN}) of 57 cm^{-1} (Figure 3); hence grafting the imidazole does not affect the Lewis acidity of the remaining Cr^{3+} CUS.

Density Functional Theory (DFT) was used to study the binding of imidazole with Cr and electrostatic potential around the Cr_3O trimer cluster (Figure S12). The Cr-imidazole binding energy was found to be 26 kcal mol^{-1} with dispersion correction, indicating its strong interaction with exposed Cr site. The fluorine atom was highly electronegative in both MIL-101(Cr) and MIL-101-Me. However, the electronic field generated near the terminal imidazole may produce another favorable adsorption site. The sorption of CO_2 was then investigated with Grand Canonical Monte Carlo (GCMC) simulations in both MIL-101(Cr) and MIL-101-Me (Table S4, S5 and Figure S13), using parameters derived from our DFT findings.
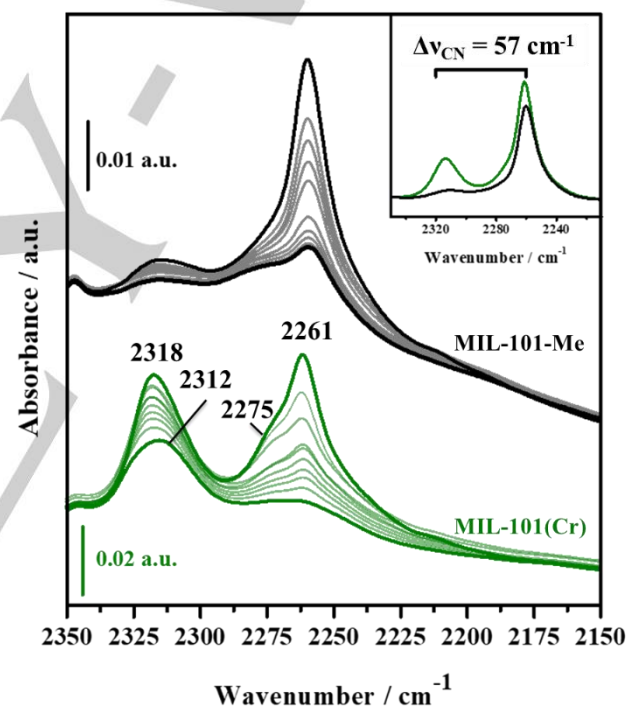

Figure 2: DR UV-Vis spectra of CO_2 adsorption (100 mbar, dotted lines) at room temperature on MIL-101(Cr) (green) and MIL-101-Me (black). Solid lines refer to samples in *vacuo* and dashed lines to the samples upon outgassing CO_2 (at RT).

In all samples, bands in the NIR and FTIR spectra due to the MIL-101(Cr) framework are present. Notably, strong absorptions in the region of 1800-1300 cm^{-1}, from the dicarboxylate linker ($v_{as}(COO)$, $v_s(COO)$ and $v(C–C)$) are seen, and at 1017 ($\delta(C-H)$) and 750 ($\gamma(C-H)$) cm^{-1} due to the aromatic rings (Figure S10).[24] In MIL-101-Me, a new band is observed at 3140 cm^{-1} is assigned to the $v(C–H)$ ring stretch of the imidazole (Figure S11A) as well as further imidazole features at 1237 and 1112 cm^{-1} for $\delta(C–H)$ in-plane and out-of-plane vibrations respectively. Each band is observed to be shifted relative to the unbound imidazole (3118 cm^{-1}, Figure S11B). Detection of the additional, imidazole-indicative bands in the FT-IR along with the first overtone of the $v(C–H)$ in the NIR region (6180 cm^{-1}, Figure S8) prove the grafting of the imidazole onto the MIL-101(Cr) CUS. To investigate the Lewis acidity of MIL-101(Cr) and MIL-101-Me, CD_3CN was used as a molecular probe (Figure 3) to study the C≡N stretching region. By decreasing the CD_3CN pressure, a weak shoulder at *ca.* 2275 cm^{-1} appears as the probe molecule

Figure 3: FTIR difference spectra of decreasing CD_3CN coverages (from vapor pressure to vacuum) of MIL-101(Cr) (green) and MIL-101-Me (black). Before adsorption, the samples were outgassed at 150 °C. The 2261 cm^{-1} signal is physisorbed CD_3CN.
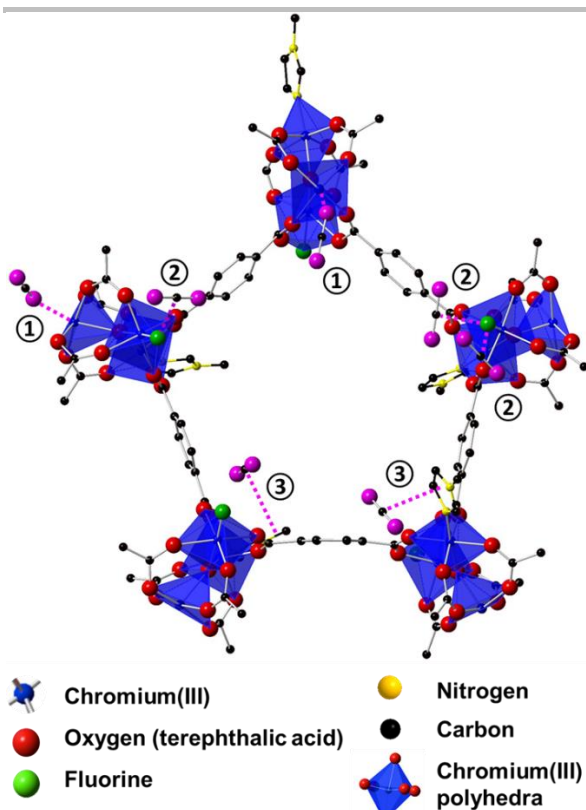
COMMUNICATION

Figure 4: GCMC simulated favorable CO_2 adsorption sites in one cross-sectional pentagonal cluster of MIL-101-Me. For illustrative purposes - framework oxygen are red, carbon dioxide oxygen are pink. Numbers 1, 2 and 3 relate to distinct binding sites with distances of 2.17, 2.43 and 3.19 Å respectively.

The generated adsorption isotherms of CO_2 at low pressure (Figure S14), show there is enhanced uptake in MIL-101-Me. To identify the precise site responsible for enhanced CO_2 binding in MIL-101-Me, simulation snapshots (Figure 4) of CO_2 located in a pentagonal windows of MIL-101(Cr) and MIL-101-Me were compared. For MIL-101(Cr), two favorable binding sites were observed. Site (1), shows an interaction between the electron poor CUS Cr atom and the oxygen of CO_2, with a corresponding Cr—OCO distance of 2.17 Å. Site (2), shows the electron rich fluorine interacting with the carbon of CO_2, at an F—CO_2 distance of 2.43 Å. Sites (1) and (2) are inherent to the framework, so are seen in MIL-101-Me also. MIL-101-Me possesses an additional adsorption site (3), attributed to the grafted imidazole moiety, which facilitates CO_2 sorption parallel to the 5-membered ring plane (Figure 4).

To quantitatively identify these adsorption sites, radial distribution functions (RDFs) of CO_2 molecules around framework atoms were calculated. Two sharp peaks are observed for Cr and F atoms (Figure S15A and B), which is consistent with the electrostatic potential maps (Figure S12) and correlate to sites (1) and (2) (Figure 4). For MIL-101-Me, peaks are observed in the RDF for the imidazole molecule with CO_2 (Figure S15C), which further substantiates the higher sorption of CO_2, when compared with MIL-101(Cr). The imidazole therefore, crucially provides an extra sorption site, (3), which favorably enhances CO_2 sorption.
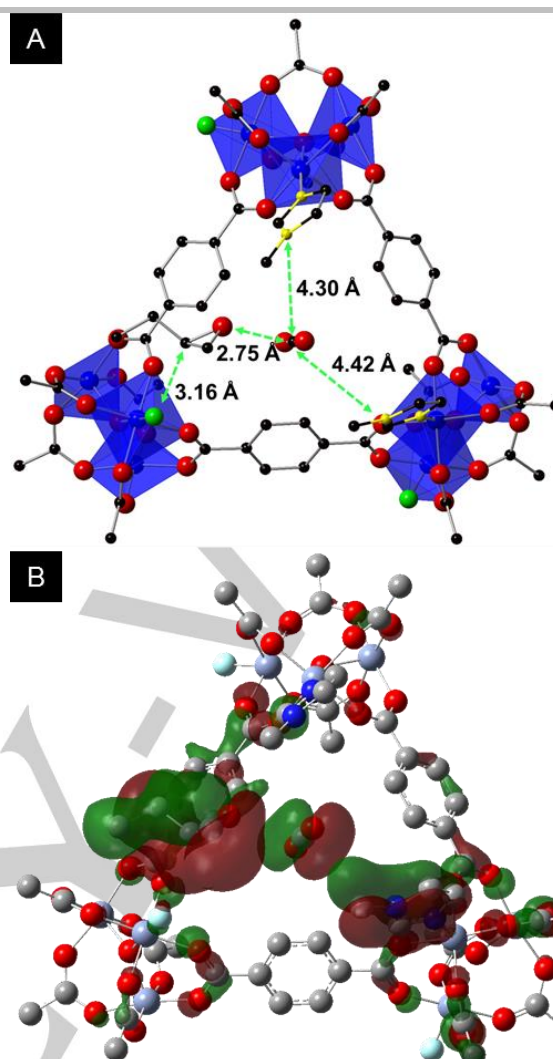

Figure 5: A) Favorable adsorption site for epoxide and CO_2 in a $(Cr_3O)_3$ cluster of MIL-101-Me calculated by DFT; a "cave" formed by two grafted Me groups and F atom is shown. B) Butylene oxide and CO_2 cluster with molecular orbitals shown.

The interactions between MIL-101-Me and a CO_2/butylene oxide mixture was investigated by both GCMC simulations and DFT calculations. DFT calculations, Figure 5, revealed that CO_2 preferentially adsorbs between grafted imidazoles, site (3), Figure 4. The epoxide is held close to the fluorine, site (2), as confirmed by the RDF (Figure S16). The distance between the CO_2 and the epoxide is 2.75 Å, (Figure 5A) bringing the two substrates (reagents) close together and so enhancing the probability of a reaction occurring. The molecular orbitals (Figure 5B) detail how both of the grafted imidazole species help to stabilize CO_2 near the epoxide *via* the π- π interactions which were observed. Strong van der Waals interactions are not seen in the MIL-101(Cr), as the substrates are further apart, which further confirms the importance of the imidazole rings in MIL-101-Me in aiding the sorption of CO_2 around the epoxide. GCMC simulations revealed very similar arrangement of both CO_2 and the epoxide, Figure S17. The RDF of the epoxide-CO_2 distances further demonstrates the enhanced propensity to form epoxide-CO_2 clusters in MIL-101-Me than in MIL-101(Cr) (Figure S18). We believe that the proximity of the imidazole and electronegative F produces enhanced CO_2 utilization, as the two reagents are brought closer together to initiate the catalytic reaction (proximity effect). The extra sorption site for CO_2 that the MIL-101-Me provides is thus crucial as without which, as is the case for MIL-101(Cr), the epoxide is favored to occupy the F and CUS sorption sites and there is no further site available for

COMMUNICATION

CO_2 occupation. A secondary cluster of CO_2 and the epoxide was also observed similar to Figure 5, but within a different aperture formed by three Cr_3O clusters containing: a grafted imidazole, an open metal site and the remaining and an F atom, Figure S19. Here, the molecular orbitals clearly show a bridge between imidazole, CO_2 and epoxide again via π- π interaction, inferring further the requirement of the imidazole to initiate the reaction between CO_2 and the epoxide.

The MIL-101-based materials were tested for the catalytic formation of butylene carbonate from 1,2-butylene oxide and CO_2 (Figure 6 and S20A). In all cases, the systems were found to be highly selective for the cyclic carbonate (> 98 mol% selectivity) under comparatively shorter reaction times than those reported in the literature (Table S1). In line with our theoretical simulations, the imidazole-functionalized MIL-101 species out-performed the bare MIL-101(Cr).[27] A consistent level of activity was seen between different imidazole species (Figure S20A), highlighting the robustness of our methodology, with all reactions going to completion within 6 hours (Figure S20B), with steady turnover frequencies (TOFs) of 553 hr^{-1}.
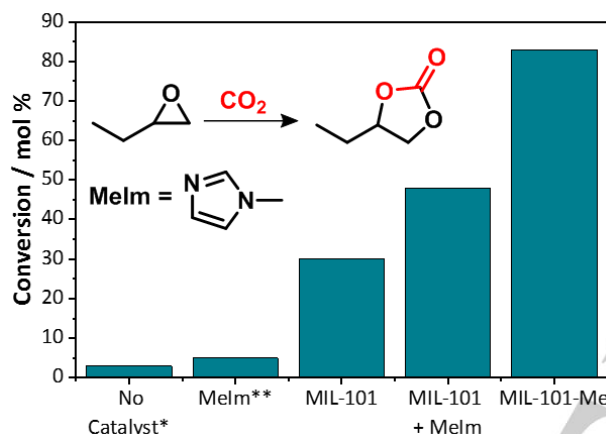

Figure 6: Conversion values of butylene oxide for the reaction with CO_2 to butylene carbonate. Reaction conditions: butylene oxide (55 mmol), catalyst MIL-101-Me (0.96 mmol/g, 0.075 mol %), solvent free, 115 °C, 1.5 hours, 2 MPa CO_2 (at RT). *Blank (no catalyst) reaction time 24 hours. **Free imidazole reaction time 6 hours.

To justify the benefits of imidazole grafting, a physical mixture of 1-methyl imidazole and MIL-101(Cr) (equimolar amounts to MIL-101-Me; "MIL-101 + MeIm" Figure 6) was tested, showing inferior catalytic performance (48 mol %) to MIL-101-Me (83 mol%, TOF 770 hr^{-1}, Figure 6). This confirms that the precise location and proximity of the imidazole and Cr^{3+} CUS is imperative for enhanced catalytic activity. It was noted that the conversion for the physical mixture is slightly larger than the sum of the MIL-101 and MeIm conversions. This is likely the result of the imidazole aiding CO_2 sorption into the reaction mixture, or binding to the CUS during catalysis. Evidence for the latter can be seen via UV-Vis of the physical mixture post-catalysis, (Figure S21A), as the d-d transitions are blue-shifted, though not to the extent of MIL-101-Me, indicative of lower loading.

On recycling (Table S6), it can be seen that MIL-101-Me does not suffer from appreciable loss in catalytic activity. Furthermore, the structural and spectroscopic properties were retained, following several catalytic cycles. SEM images after catalysis (Figure S22), show minimal changes in the particle morphology and size. Similarly, DR UV-Vis (Figure S21B) showed imidazole anchoring is retained post-catalysis, as the shift in peak positions is still discernable when compared with MIL-101(Cr). These findings further confirm and vindicate the importance of the heterogeneous nature of the imidazole-grafted MIL-101 system.

The grafting of imidazole species to the Cr^{3+} CUS of MIL-101(Cr) framework affords a highly active and selective catalyst for CO_2 utilization, under halide-free and solvent-free conditions. The availability of coordinatively unsaturated sites provides unique handles for isolating the functionalized imidazole species, removing the need for a co-catalyst. The site-isolation of the imidazole, leads to high turnover frequencies and substantially reduced reaction times, making the methodology industrially attractive. More importantly, molecular simulations show that the specific binding of the imidazole to the coordinatively unsaturated chromium species brings the epoxide in close proximity to the CO_2, which plays a significant role in improving the ensuing catalytic activity. It is envisaged that the additional binding site introduced on the functionalized imidazole catalyst, allied with the pre-existing Lewis sites, as evidenced from the spectroscopic studies, facilitates epoxide activation[26] and stabilizes reaction intermediates, leading to enhanced CO_2 utilization. Our approach offers adequate scope for extending the design rationale for the chemical fixation of CO_2, via the copolymerization with epoxides, to afford polycarbonates.[27]

REFERENCES

[1]   M. H. Beyzavi, C. J. Stephenson, Y. Liu, O. Karagiaridi, J. T. Hupp, O. K. Farha, *Front. Energy Res.* **2015**, *2*.
[2]   J. W. Maina, C. Pozo-Gonzalo, L. Kong, J. Schütz, M. Hill, L. F. Dumée, *Mater. Horiz.* **2017**, *4*, 345.
[3]   A. Dhakshinamoorthy, A. M. Asiri, M. Alvaro, H. Garcia, *Green Chem.* **2018**, *20*, 86.
[4]   G. Férey, C. Mellot-Draznieks, C. Serre, F. Millange, J. Dutour, S. Surblé, I. Margiolaki, *Science* **2005**, *309*, 2040.
[5]   X. Kong, E. Scott, W. Ding, J. A. Mason, J. R. Long, J. A. Reimer, *J. Am. Chem. Soc.* **2012**, *134*, 14341.
[6]   Y. K. Hwang, D.-Y. Hong, J.-S. Chang, S. H. Jhung, Y.-K. Seo, J. Kim, A. Vimont, M. Daturi, C. Serre, G. Férey, *Angewandte Chemie International Edition* **2008**, *47*, 4144.
[7]   Q. Luo, M. Ji, M. Lu, C. Hao, J. Qiu, Y. Li, *J. Mater. Chem. A* **2013**, *1*, 6530.
[8]   S. M. J. Rogge, A. Bavykina, J. Hajek, H. Garcia, A. I. Olivos-Suarez, A. Sepúlveda-Escribano, A. Vimont, G. Clet, P. Bazin, F. Kapteijn, M. Daturi, E. V. Ramos-Fernandez, F. X. L. i Xamena, V. V. Speybroeck, J. Gascon, *Chem. Soc. Rev.* **2017**, *46*, 3134.
[9]   J. M. Thomas, R. Raja, D. W. Lewis, *Angewandte Chemie International Edition* **2005**, *44*, 6456.
[10]   P.-Z. Li, X.-J. Wang, J. Liu, J. S. Lim, R. Zou, Y. Zhao, *J. Am. Chem. Soc.* **2016**, *138*, 2142.
[11]   L. Liang, C. Liu, F. Jiang, Q. Chen, L. Zhang, H. Xue, H.-L. Jiang, J. Qian, D. Yuan, M. Hong, *Nat Commun* **2017**, *8*, 1233.
[12]   V. Guillerm, Ł. J. Weseliński, Y. Belmabkhout, A. J. Cairns, V. D'Elia, Ł. Wojtas, K. Adil, M. Eddaoudi, *Nature Chemistry* **2014**, *6*, 673.
[13]   W.-Y. Gao, Y. Chen, Y. Niu, K. Williams, L. Cash, P. J. Perez, L. Wojtas, J. Cai, Y.-S. Chen, S. Ma, *Angew. Chem. Int. Ed. Engl.* **2014**, *53*, 2615.
[14]   J. Liang, R.-P. Chen, X.-Y. Wang, T.-T. Liu, X.-S. Wang, Y.-B. Huang, R. Cao, *Chem. Sci.* **2017**, *8*, 1570.
[15]   J. Liang, Y.-Q. Xie, X.-S. Wang, Q. Wang, T.-T. Liu, Y.-B. Huang, R. Cao, *Chem. Commun.* **2018**, *54*, 342.
[16]   L.-G. Ding, B.-J. Yao, W.-L. Jiang, J.-T. Li, Q.-J. Fu, Y.-A. Li, Z.-H. Liu, J.-P. Ma, Y.-B. Dong, *Inorg. Chem.* **2017**, *56*, 2337.
[17]   D. Liu, G. Li, H. Liu, *Applied Surface Science* **2018**, *428*, 218.
[18]   Y. Wu, X. Song, S. Xu, J. Zhang, Y. Zhu, L. Gao, G. Xiao, *Catal Lett* **2019**, *149*, 2575.

WILEY-VCH

COMMUNICATION

[19] D. Scarano, G. Spoto, S. Bordiga, L. Carnelli, G. Ricchiardi, A. Zecchina, *Langmuir* **1994**, *10*, 3094.

[20] B. M. Weckhuysen, I. E. Wachs, R. A. Schoonheydt, *Chem. Rev.* **1996**, *96*, 3327.

[21] A. Vimont, J.-M. Goupil, J.-C. Lavalley, M. Daturi, S. Surblé, C. Serre, F. Millange, G. Férey, N. Audebrand, *J. Am. Chem. Soc.* **2006**, *128*, 3218.

[22] R. L. Puurunen, B. M. Weckhuysen, *Journal of Catalysis* **2002**, *210*, 418.

[23] X. Wang, H. Li, X.-J. Hou, *J. Phys. Chem. C* **2012**, *116*, 19814.

[24] N. V. Maksimchuk, M. N. Timofeeva, M. S. Melgunov, A. N. Shmakov, Yu. A. Chesalov, D. N. Dybtsev, V. P. Fedin, O. A. Kholdeeva, *Journal of Catalysis* **2008**, *257*, 315.

[25] M. Boronat, P. Concepción, A. Corma, M. Renz, S. Valencia, *Journal of Catalysis* **2005**, *234*, 111.

[26] D. Ma, B. Li, K. Liu, X. Zhang, W. Zou, Y. Yang, G. Li, Z. Shi, S. Feng, *J. Mater. Chem. A* **2015**, *3*, 23136.

[27] D. J. Stewart, R. Raja, PCT/GB2019/053596, An invention for the use of a modulated hybrid catalyst for the conversion of CO2 to polycarbonates, December **2019**

WILEY-VCH

COMMUNICATION

Entry for the Table of Contents

Layout 1:

COMMUNICATION

Metal organic frameworks, modified with imidazole linkers in close proximity to the metal nodes, have been shown to be highly active for the utilisation of CO_2 to cyclic carbonates. A combination of spectroscopy and theoretical calculations reveal the nature of the active sites and associated catalytic mechanism validating the design of modified MIL-101(Cr).

CO_2

MIL-101-Me
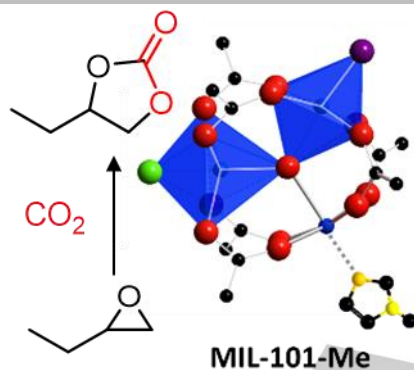
William R. Webb, Matthew E. Potter, Daniel J. Stewart, Stuart J. Elliott, Pier J. A. Sazio, Zhongxing Zhang, He-Kuan Luo, Jinghua Teng, Liling Zhang, Chiara Ivaldi, Ivana Miletto, Enrica Gianotti and Robert Raja*

Page No. – Page No.

The significance of metal coordination in imidazole-functionalized metal organic frameworks for carbon dioxide utilization